CSI-CFI Formulations of the Multiresolution Inexact Newton Method – A Numerical Comparison

***Giacomo Oliveri*[1], *Andrea Randazzo*[2], *Matteo Pastorino*[2], and *Andrea Massa*[1]**

[1]Eledia Research Group@DISI, University of Trento, 38123 Trento, Italy
Phone: +39 0461 882057, Fax: +39 0461 882063
Email: giacomo.oliveri@disi.unint.it, andrea.massa@ing.unitn.it

[2]Department of Biophysical and Electronic Engineering, University of Genoa, 16100 Genoa, Italy
Phone: +39 010 353 2242, Fax: +39 010 353 2245
Email: andrea.randazzo@unige.it, matteo.pastorino@unige.it

Abstract

A numerical comparison of two innovative microwave imaging strategies is presented. To effectively tackle the non-linearity and ill-posedness arising in the inversion process, the techniques integrate a multi-resolution approach with two different 'Inexact-Newton' methods developed either within the contrast source or within the contrast field formulations of the inverse scattering problem. A set of preliminary numerical results is presented to compare the features and potentialities of the methods.

1. Introduction and Motivation

In the last years, great efforts have been devoted to the development of fast and efficient electromagnetic imaging techniques [1]-[7]. Indeed, inverse-scattering methods are gaining a lot of attention due to their applicability to several technological domain, such as non-destructing testing and evaluations in civil and industrial fields, medical imaging, and subsurface inspection [1]-[7]. In such approaches, the objects under analysis are illuminated by means of known "incident" electromagnetic fields, and the response to such interrogation, i.e., the 'scattered field', is recorded [1]. Microwave imaging methods aim at obtaining a reconstruction of the dielectric properties of the investigated region starting from the measured samples of such field [1]-[7].

In this framework, the inverse scattering problem is usually formulated in terms of two electric field integral equations, which relate the measured scattered electric field (*data term*) and the incident electric field (*state term*) to the distributions of the dielectric properties and of the electric field in the investigation area (*CFI* formulation). However, alternative formulations have been proposed as well [8]. Indeed, the microwave imaging problem has been more recently stated in terms of the contrast source integral equations whose unknowns are the induced current (i.e., the contrast source) and the contrast function (*CSI* formulation) [8]. Such approaches have been actually proposed since the resulting problem exhibit a *linear* data equation, thus yielding a simpler problem to be solved. Unfortunately, both *CSI*- and *CFI*-formulated inverse scattering problems turn out to be non linear and severely ill-posed, therefore yielding to several theoretical/numerical issues in their solutions.

Several techniques have been proposed in the recent years to mitigate such features. More specifically, multi-resolution strategies proved to be very effective in reducing the local-minima problems [10, 11]. Moreover, efficient regularization techniques able to mitigate the ill-posedness/ill-conditioning of the involved equations, such as Inexact-Newton-based methods [9][12], have been investigated by using the two formulations previously introduced. To efficiently tackle both the ill-posedness and the local-minima issues, the integration of regularization and multi-scaling strategies has also been preliminarily discussed for the *CFI* formulation [13].

In the present paper, the inversion strategy developed in [13] (denoted as *IMSA-IN-CFI*) is further analyzed and a new multi-resolution approach based on the CSI formulation (denoted as *IMSA-IN-CSI*) is briefly introduced. The performances of the two methods are evaluated and compared by means of a preliminary set of numerical simulations.

2. Mathematical formulation

A cylindrical unknown scatterer is located inside a known investigation area A_{inv}, whose background is composed by a linear and isotropic homogeneous medium with complex dielectric permittivity ε_b and magnetic permeability $\mu_b = \mu_0$ (being μ_0 the magnetic permeability of the vacuum.). The object is illuminated by a TM incident

978-1-4244-6051-9/11/$26.00 ©2011 IEEE

electric field with z-component denoted as $E_{inc}(\mathbf{r})$, which in the present paper is supposed to be generated by a line-current source located at positions $\mathbf{r}_{ill}$. Since under the previous assumptions the scattering problem can be described in terms of scalar 2D equations, in the following all the field quantities are representative of the z-components of the electric fields. Moreover, a $e^{j\omega t}$ time dependence is assumed and omitted in the following. The electric field scattered by the object, $E_{scatt}(\mathbf{r})$, is collected in a measurement domain A_{meas}, which in a discrete setting is composed by M points, located at $\mathbf{r}_{meas}^{(m)}$. For the sake of simplicity, the mathematical formulation presented in this paper is referred to a single view case; the multi-view extension is straightforward and can be found in several papers (e.g., [8][11].)

As it is well known, the measured electric field can be related to the dielectric properties of the investigation area by means of a non-linear operator equation [1], i.e.,

$$\mathbf{y} = \mathbf{\Lambda}(\mathbf{x}) \tag{1}$$

where **x** and **y** contain the unknown functions to be retrieved and the measured and/or known functions, respectively.

In the standard CFI formulation [1], the known term is given by $\mathbf{y} = \begin{bmatrix} E_{scatt} & E_{inc} \end{bmatrix}^t$, being the superscript t the transpose operator and E_{inc} the incident electric field inside the investigation area, whereas the unknown vector **x** is $\mathbf{x} = \begin{bmatrix} \tau & E_{tot} \end{bmatrix}^t$, where E_{tot} is the total electric field inside the investigation domain and τ is the contrast function, defined as

$$\tau(\mathbf{r}) = \varepsilon(\mathbf{r})/\varepsilon_b - 1\,,\ \ \mathbf{r} \in A_{inv} \tag{2}$$

In equation (2), $\varepsilon(\mathbf{r})$ is the complex dielectric permittivity at point $\mathbf{r} \in A_{inv}$. Moreover, the scattering operator is given by $\mathbf{\Lambda}^{CFI}(\mathbf{x}) = \begin{bmatrix} \Lambda_{ext}^{CFI}(\mathbf{x}) & \Lambda_{int}^{CFI}(\mathbf{x}) \end{bmatrix}^t$, where [1]

$$\begin{aligned} \Lambda_{ext}^{CFI}(\mathbf{x})(\mathbf{r}) &= -k^2 \int_{A_{inv}} \tau(\mathbf{r}')E_{tot}(\mathbf{r}')g(\mathbf{r},\mathbf{r}')d\mathbf{r}', \quad \mathbf{r} \in A_{meas} \\ \Lambda_{int}^{CFI}(\mathbf{x})(\mathbf{r}) &= E_{tot}(\mathbf{r}) + k^2 \int_{A_{inv}} \tau(\mathbf{r}')E_{tot}(\mathbf{r}')g(\mathbf{r},\mathbf{r}')d\mathbf{r}', \quad \mathbf{r} \in A_{inv} \end{aligned} \tag{3}$$

In the CSI formulation, the known and unknown terms are $\mathbf{y} = \begin{bmatrix} E_{scatt} & 0 \end{bmatrix}^t$ and $\mathbf{x} = \begin{bmatrix} \tau & J \end{bmatrix}^t$, respectively, where J is the so-called contrast source [7] given by $J(\mathbf{r}) = \tau(\mathbf{r})E_{tot}(\mathbf{r})$, $\mathbf{r} \in A_{inv}$. In this case, the scattering operator is given by $\mathbf{\Lambda}^{CSI}(\mathbf{x}) = \begin{bmatrix} \Lambda_{ext}^{CSI}(\mathbf{x}) & \Lambda_{int}^{CSI}(\mathbf{x}) \end{bmatrix}^t$, where [9]

$$\begin{aligned} \Lambda_{ext}^{CSI}(\mathbf{x})(\mathbf{r}) &= -k^2 \int_{A_{inv}} J(\mathbf{r}')g(\mathbf{r},\mathbf{r}')d\mathbf{r}', \quad \mathbf{r} \in A_{meas} \\ \Lambda_{int}^{CSI}(\mathbf{x})(\mathbf{r}) &= J(\mathbf{r}) - \tau(\mathbf{r})E_{inc}(\mathbf{r}) + k^2\tau(\mathbf{r}) \int_{A_{inv}} J(\mathbf{r}')g(\mathbf{r},\mathbf{r}')d\mathbf{r}', \quad \mathbf{r} \in A_{inv} \end{aligned} \tag{4}$$

3. Inexact-Newton iterative multi-scaling approach

In the approach presented in this paper, equation (1) is solved by means of an iterative multi-scaling strategy. At each stage of the *IMSA*, the involved equations are discretized by subdividing the investigation domain into N cells according to the Richmond's procedure. Consequently, a set of S discrete inverse problems $\mathbf{y}^{(s)} = \mathbf{\Lambda}^{(s)}(\mathbf{x}^{(s)})$, $s = 1, \ldots, S$, is obtained, being S the number of IMSA stages.

In the *IMSA-IN* framework, the solution of the inverse scattering problem at the sth step is obtained by means of the following iterative procedure [13]

1. Set $n = 0$ and initialize the unknown $\mathbf{x}_n^s$ with the reconstruction obtained at the previous step
2. Linearize equation (1), in order to obtain a linear equation $\mathbf{\Lambda}'_{\mathbf{x}_n^s}\delta\mathbf{x}_n^s = \mathbf{y}^s - \mathbf{\Lambda}(\mathbf{x}_n^s)$, being $\mathbf{\Lambda}'_{\mathbf{x}_n^s}$ the Frechet derivative of $\mathbf{\Lambda}$ at point $\mathbf{x}_n^s$ [9][12]. The operator to be used depends upon the considered formulation ($\mathbf{\Lambda}^{CFI}$ for the CFI formulation and $\mathbf{\Lambda}^{CSI}$ for the CSI formulation).

3. Find a regularized solution $\delta\tilde{\mathbf{x}}_n^s$ to the linearized equation by using a truncated Landweber algorithm (stopped after I_{IN} iterations).
4. Update current solution with $\mathbf{x}_{n+1}^s = \mathbf{x}_n^s + \delta\tilde{\mathbf{x}}_n^s$
5. Repeat steps (2)-(4) until a predefined stopping criterion is satisfied (e.g., a maximum number of iterations I_{out} is reached.)

The reconstructed dielectric profile at the *s*th scale is filtered and clustered in order to define the regions of interest (i.e., those where the object is located by the inversion method). After such regions are identified, the discretization grid is refined to deduce the updated version of equation (1) at the *s+1* step [10]. The *IMSA-IN* is iterated until a predefined stopping rule is satisfied (e.g., the size and location of the region of interest does not change) [10].

4. Numerical Results

A numerical analysis is presented in this section to compare the features of the considered *IMSA−IN* based methods. Towards this end, an investigation domain of size $2.4\lambda \times 2.4\lambda$ (free-space background) is illuminated by *V*=24 TM-waves. The total field calculated through a *MoM*-based solver (by exploiting different discretization grids in the direct and inverse procedures in order to avoid the "inverse-crime" problem) has been collected at *M*=24 measurement points located on a circle of radius 1.8*λ*, and the inversion procedures have been carried out assuming $I_{in} = I_{out} = 30$ and *S*=4.

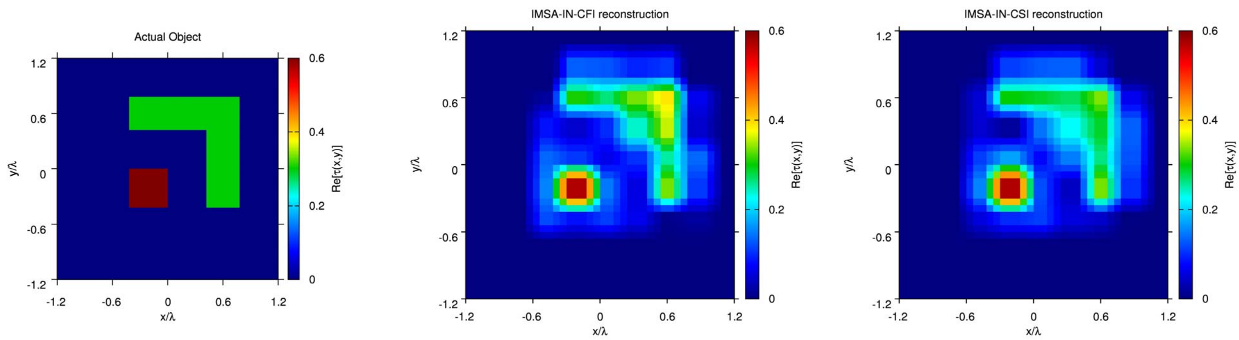

(*a*) (*b*) (*c*)

Figure 1. [*Separate Cylinders*, *SNR*=30 dB] Actual (*a*) and retrieved dielectric profiles by (*b*) *IMSA-IN-CFI* and (*c*) *IMSA-IN-CSI*.

In the first numerical example, two lossless scatterers with different permittivity ($\tau_{square} = 0.6$, $\tau_{l-shaped} = 0.3$) are considered [Fig. 1(*a*)]. The *IMSA-IN-CFI* and *IMSA-IN-CSI* retrieved contrast profiles assuming a signal-to-noise ratio *SNR* of 30 dB show that (*a*) both methods are able to correctly detect the presence of two separate objects as well as to identify their shapes [Fig. 1(*b*) vs. 1(*c*)]; (*b*) however, the *CSI*-based inversion method provides a more accurate estimation of the object contrasts (specifically, regarding the "*L-shaped*" object [Fig. 1(*c*)].

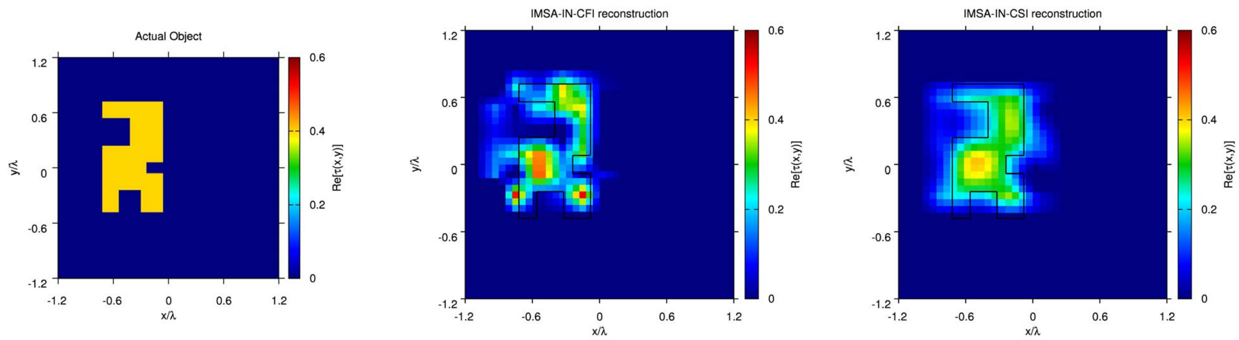

(*a*) (*b*) (*c*)

Figure 2. [*Irregular Cylinder*, *SNR*=10 dB] Actual (*a*) and retrieved dielectric profiles by (*b*) *IMSA-IN-CFI* and (*c*) *IMSA-IN-CSI*.

The enhanced accuracy of the *IMSA-IN-CSI* turns out even more evident when dealing with lower *SNR* scenarios. To investigate this feature, the next numerical experiment concerns a dielectric scatterer characterized by the τ profile in Fig. 2(*a*). The retrieved contrast functions assuming *SNR*=10 dB (Fig. 2) show that, despite an expected accuracy reduction (due to the *SNR* value), the *IMSA-IN-CSI* is able to correctly detect the location and shape of the object [Fig. 2(*c*)], while, on the contrary, the *IMSA-IN-CFI* yields to a low quality reconstruction with some strong artifact [Fig. 2(*b*)].

5. Conclusion

A preliminary numerical comparison of the features and potentialities of two multi-resolution microwave imaging techniques based on the Inexact-Newton approach has been presented. The reported results indicate that, while the two methods yield to a similar accuracy when high *SNR* conditions are at hand, the *CSI*-based procedure outperforms the *CFI* one when dealing with strongly corrupted data. A comparison of the computational complexity of the two methods as a function of the view and measurement number and of the investigation domain size is currently under investigation.

6. References

1. M. Pastorino, *Microwave Imaging*. Hoboken, NJ: John Wiley & Sons, 2010.

2. R. Zoughi, *Microwave Nondestructive Testing and Evaluation*. The Netherlands: Kluwer Academic Publishers, 2000.

3. P. Rocca, M. Benedetti, M. Donelli, D. Franceschini, and A. Massa, “Evolutionary optimization as applied to inverse scattering problems”, *Inverse Problems*, vol. 25, no 6, pp. 1-41, art. no. 123003, Dec. 2009.

4. A Massa, M Pastorino, and A Randazzo, “Reconstruction of two-dimensional buried objects by a differential evolution method,” *Inverse Problems*, vol. 20, no. 6, pp. S135–S150, Dec. 2004.

5. S. Caorsi, A. Massa, and M. Pastorino, “A computational technique based on a real-coded genetic algorithm for microwave imaging purposes,” *IEEE Trans. Geosci. Remote Sens*., vol. 38, no. 4, pp. 1697-1708, Jul. 2000.

6. M. Donelli and A. Massa, “A computational approach based on a particle swarm optimizer for microwave imaging of two-dimensional dielectric scatterers,” *IEEE Trans. Microwave Theory Tech*., vol. 53, no. 5, pp. 1761-1776, May 2005.

7. P. M. Meaney, M. W. Fanning, D. Li, S. P. Poplack, and K. D. Paulsen, “A clinical prototype for active microwave imaging of the breast,” *IEEE Trans. Microwave Theory Tech.*, vol. 48, pp. 1841-1853, Nov. 2000.

8. P. M. van den Berg and A. Abubakar, “Contrast source inversion method: State of art,” *Progress Electromagn. Res.*, vol. 34, pp. 189–218, 2001.

9. G. Bozza and M. Pastorino, “An inexact Newton-based approach to microwave imaging within the contrast Source Formulation,” *IEEE Trans. Antennas Propagat.*, vol. 57, no. 4, pp. 1122-1132, Apr. 2009.

10. S. Caorsi, M. Donelli, D. Franceschini, and A. Massa, “A new methodology based on an iterative multiscaling for microwave imaging,” *IEEE Trans. Microwave Theory Tech.*, vol. 51, no. 4, pp. 1162-1173, Apr. 2003.

11. S. Caorsi, M. Donelli, and A. Massa, “Detection, location, and imaging of multiple scatterers by means of the iterative multiscaling method,” *IEEE Trans. Microwave Theory Tech.*, vol. 52, pp. 1217-1228, Apr. 2004.

12. G. Bozza, C. Estatico, A. Massa, M. Pastorino, and A. Randazzo, “Short-range image-based method for the inspection of strong scatterers using microwaves,” *IEEE Trans. Instrum. Meas.*, vol. 56, no. 4, pp. 1181-1188, Aug. 2007.

13. G. Oliveri, G. Bozza, A. Massa, and M. Pastorino, “Iterative multi scaling-enhanced Inexact Newton-method for microwave imaging,” *Proc. IEEE-APS/URSI 2010*, pp. 1-4, 11-17 Jul. 2010.